

HOUSKA BASED TIME-DEPENDENT RHEOLOGICAL MODEL FOR FLOCCULATED TAILINGS

Arno Talmon¹, Ebi Meshkati²

DOI: 10.30825/4.14-15.2023

¹*Delft University of Technology & Deltares, Mekelweg 2, 2628 CD, Delft, The Netherlands,
a.m.talmon@tudelft.nl, arno.talmon@deltares.nl*

²*Deltares (now with R&D Boskalis, Rosmolenweg 20, 3356 LK, Papendrecht, The Netherlands,
ebi.meshkati@boskalis.com)*

ABSTRACT: The rheology of tailings depends on composition and is shear- and time-dependent. Time-dependency might be at the origin of phenomena such as channel and pattern formation in tailings beaching. Rheology is governed by colloids that form a structure within the fluid. This paper concerns the fitting of the Houska rheological model to controlled stress rheometry data of polymer treated material. The Houska model describes reversible time-dependency, e.g., thixotropy. A novelty here is that irreversible shear down (rheomalaxis) is added to the thixotropy originally captured by the model. The Houska model has the advantage that its time-dependency can be phase-wise implemented and tested in numerical codes. In our study, it is shown how the model can be fitted to published detailed controlled shear stress rheometry on flocculated mature fine tailings and is compared with the fitting by a viscosity bifurcation model, which was originally applied. The fits of the viscosity bifurcation model and the current model are comparable. The influence of rheomalaxis on the formation of a lubricating layer in tailings disposal on a beach is investigated by means of a CFD model: flow depth reduces and irregular flow develops.

KEY WORDS: clays, thixotropy, rheomalaxis, constitutive model, CFD.

NOTATION

a & b	constants for growth and decay of structure [1/s] & [-]
c	increment of viscosity index for fully structured fluid [Pa]
E	cumulative shear energy dissipation per unit volume [kJ/m ³]
$E_{63\%}$	cumulative shear energy dissipation at 63% decay of structure [kJ/m ³]
I	inertia [s]
n	flow index [-]
q	flow rate per unit width [m ² /s]
β	b/a [s]
$\dot{\gamma}$	shear rate [1/s]
$\dot{\gamma}_0$	reference shear rate [1/s]
λ	structure parameter [0- λ_0]
λ_0	maximum value of structure [0-1]

$\lambda_{0\infty}$	maximum value of structure when irreversibly fully sheared down [-]
μ_b	viscosity index total destructured fluid (=Bingham plastic viscosity if $n=1$) [Pa s^n]
τ	shear stress [Pa]
τ_0	yield stress of fully structured fluid (occurs at $\lambda = 1$) [Pa]
τ_∞	yield stress of totally destructured fluid (occurs at $\lambda = 0$) [Pa]

1. INTRODUCTION

Tailings are being thickened to save water, accelerate pond reclamation, and reduce tailings pond size. In oil sands, mature fine tailings accumulated in tailing ponds are nowadays harvested and reprocessed with flocculants to improve dewatering substantially, but flocculation also affects rheology. The authors measured the rheology of a blend of mature fine tailings (MFT's) treated with polymer (Talmon et al., 2021b). But applying fundamentally different measuring protocols. Mizani et al. (2017) already measured the time-dependent rheological behaviour of flocculated mature fine tailings (f-MFT). Applying stress-controlled rheology tests (CSS), they showed how the viscosity of flocculated tailings may bifurcate (an existence of a high and a low viscosity at the same shear stress). In characterization, they adopt and adapt the Hewitt and Balmforth (2013) model, describing the reversible time-dependent behaviour of the rheology.

Flocculated tailings, however, also display irreversible time-dependency (Salinas et al., (2009); Gillies et al., (2012); Diep et al., (2014) and Neelakantan et al., (2018)). These studies show that cumulative dissipated shear energy is the governing parameter for quantification of the irreversible decay of tailings strength and rheology.

For clay suspensions in the natural environment, which generally display only reversible time-dependent behaviour, the mathematical characterisation of time-dependent behaviour is based on the original ideas of Moore (1959). Worrall-Tuliani (1964) developed a model for the equilibrium flow curve on the basis of thixotropy theory. A further development in thixotropy modelling was conducted by Houska (1981). The Houska model is basically a Herschel-Bulkley model with additions for the time- and transient state-dependent structure of the fluid. Toorman (1997) also developed a thixotropy model based on the Worrall-Tuliani approach.

In this paper, a modelling approach is presented encompassing reversible time-dependency and irreversible shear down of structure (e.g., thixotropy and rheomalaxis). The work ultimately aims to be able to better predict flow depth and areas covered when tailings are disposed in disposal areas.

This approach constitutes a new angle on the modelling of the rheology of flocculated tailings, in agreement with reported behaviours in the literature and is suitable for implementation in CFD codes solving fluid flow, and can be coded as an add-on to established shear thinning rheological models such as the Bingham, Power law, and Herschel-Bulkley models.

2. THEORY

Evolving structure is modeled and is subsequently connected to the rheology's constitutive equation.

2.1. KINETIC STRUCTURE EQUATION

The influence of the flocculated/aggregated structure of the clays on the rheology is mathematically described via the structure parameter λ , which represents the firmness of floc/aggregate structure. Growth and decay of structure are described by the kinetic rate equation for structure (originally proposed by Moore (1959), but originally with $\lambda_0=1$), following fluid parcels:

$$\frac{D\lambda}{Dt} = a(\lambda_0 - \lambda) - b\lambda\dot{\gamma} \quad (1)$$

The first term on the right-hand side describes the self-recovery of flocculation (Brownian motion and attractive forces). The second term describes the shear down of floc structure and can be shown to be related to energy dissipation. Basically, decay and recovery processes are superpositioned. The influence of reaggregation (or re-flocculation) in shear (Mietta et al. (2009), Sun (2018)) is not described by this equation and is left out of consideration in this study.

In the following, we will use the maximum structure parameter λ_0 as a variable representing the effects of irreversible shear down (Winterwerp 2017), Sect. 2.2.

2.2. IRREVERSIBLE BREAKDOWN

An example of the reduction of peak shear stress, measured in creep tests on samples that had dissipated different amounts of energy in shearing, is given in Figure 1. Diep et al., (2014), measured peak shear stress as well as the Bingham yield stress of thickened tailings to decrease with cumulative dissipated shear energy.

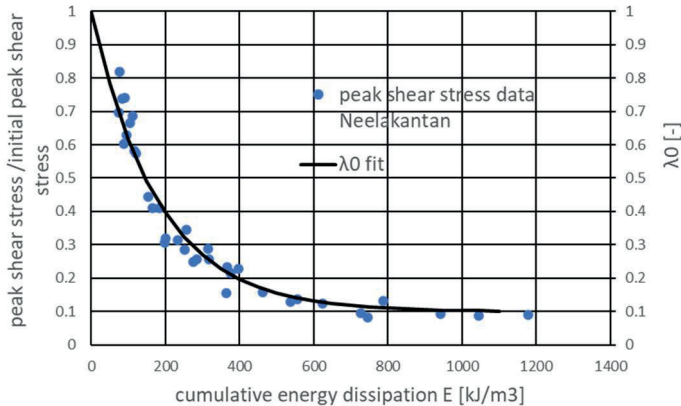


Figure 1 Sheared down rheology. Normalised peak shear stress as a function of cumulative dissipated energy. The energy is dissipated in shearing at a constant shear rate, Neelakantan et al. 2018 and negative exponential fit for λ_0

In our modelling, only the maximum value of structure, λ_0 is assumed to be reduced by irreversible shear down: the maximal attainable structure is lost, but the Bingham yield stress at $\lambda=0$ remains unchanged.

We assume that the maximum structure parameter λ_0 is linearly related to peak shear stress. Its mathematical representation, fitting the data series as shown in Figure 1, is:

$$\lambda_0 = \lambda_{0\infty} + (1 - \lambda_{0\infty})e^{-E/E_{63\%}} \quad \text{with: } E = \int_0^t \tau \dot{\gamma} dt \quad [\text{J/m}^3] \quad (2) (3)$$

Measurements of Neelakantan et al. (2018) on flocculant dosed kaolinite shown in Figure 1 characterise by $E_{63\%} = 180 \text{ [kJ/m}^3\text{]}$. Measurements by Salinas et al. (2009) on flocculated copper tailings have about the same value for $E_{63\%}$. Gillies et al. (2012) measured the rheology of flocculated oil sand tailings in pipeline transport, including initial yield stress, rate of yield stress reduction, and equilibrium (fully-sheared) yield stress. These measurements characterise by $E_{63\%} = 2000 \text{ [kJ/m}^3\text{]}$, but the yield stress is not sheared down as much as in the other research. Fitted values for $E_{63\%}$ indicate that structure decay may occur quickly in rotoviscometer tests on flocculated tailings.

2.3. RHEOLOGICAL CHARACTERISATION INCLUDING STRUCTURE

The mathematical expression of the Houska equation of state (flow curve) reads:

$$\tau = \tau_\infty + \lambda(\tau_0 - \tau_\infty) + (\mu_\infty + \lambda c)\dot{\gamma}^n \quad (4)$$

The first two terms on the right-hand side quantify the yield stress of the material. The elementary construction of the model is shown in Figure 2 by means of its constant structure curves (CSC's) and its equilibrium flow curve (EFC).

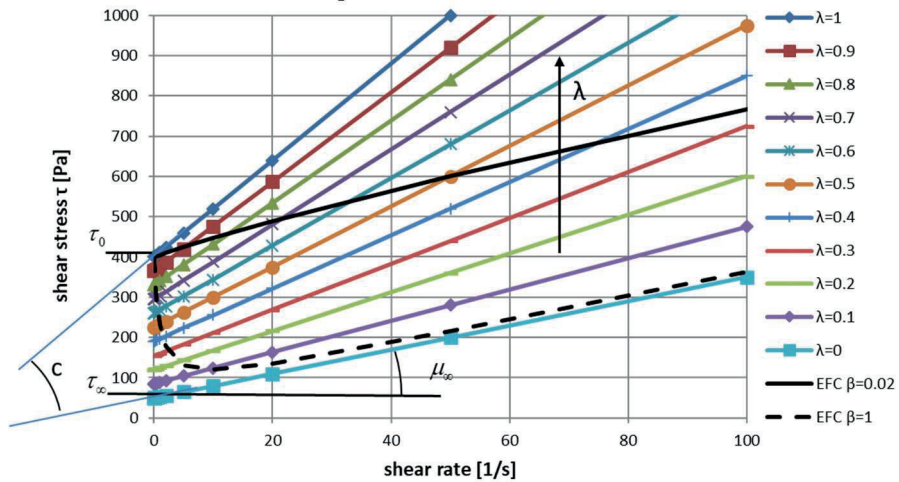


Figure 2 Example of Houska model in Bingham configuration ($n=1$, $c=9 \text{ [Pa s]}$, $\mu_\infty=3 \text{ [Pa s]}$, $\tau_0=400 \text{ [Pa]}$, $\tau_\infty=50 \text{ [Pa]}$, showing constant structure (λ) curves (CSC) and equilibrium flow curves EFC drawn for $\beta=b/a=0.02$ and $b/a=1 \text{ [s]}$)

At the EFC the growth and decay terms in Eq. (1) are equal: the structure is in equilibrium. Two different equilibrium flow curves (EFC), for the same bundle of CSC's, are shown in Figure 2. The ratio of growth and decay terms of both EFC's is different. The EFC at $b/a = \beta = 1$, depicted in Figure 2, with its distinct negative sloping branch, represents a strong thixotropic character, where the material is already recovering whilst being sheared. At high shear rates, when the fluid is entirely destructured, the Herschel-Bulkley flow curve is effectively retrieved asymptotically. Hence, associated parameters carry the subscript ∞ .

The yield stresses in the Houska model relate to the static and dynamic yield stress. The static yield stress ($\sim \tau_0$) is defined as the minimum stress required for initiating the (shear) flow in a stagnant material under stress. The yield stress of totally destructured fluid τ_{∞} is by approximation, the dynamic yield stress: defined as the minimum stress required for maintaining a given material in flow, see also Meshkati et al. (2021).

Modelling the irreversible component by a reduction of maximum structure λ_0 , Section 2.2, implies that the span of the rheological domain will shrink as a function of cumulative energy dissipation.

3. SIMULATION OF CSS RHEOMETRY

To facilitate viscosity bifurcation (create two stable solutions) into: 1) solid-like unsheared material and 2) shear flow at the same yield stress, and have solutions for shear stresses below the yield stress, viscosity regularisation (high viscosity modelling at shear stresses below the yield stress) is a necessity. To allow analytical explicit calculation of shear rate, at imposed shear stress (solving a cubic equation in $\sqrt{\dot{\gamma}}$ by Cardano's 16th century mathematical method), the yield stress terms in Eq.(4) were for simplicity multiplied by: $\sqrt{\dot{\gamma}} / (\sqrt{\dot{\gamma}} + \sqrt{\dot{\gamma}_0})$, for viscosity regularisation.

The inertia of the rotoviscometer may have played a role. In CSS simulations, the fluid shear rate is hence led to lag behind with respect to the fluid shear rate calculated according to the Houska model by means of: $\dot{\gamma} + I \partial \dot{\gamma} / \partial t = \dot{\gamma}_{Houska}$, where $\dot{\gamma}_{Houska}$ is the fluid shear rate calculated by equations (1) and (4) in CSS mode. I is a relaxation time scale representing the inertia of the rotoviscometer.

3.1. REVERSIBLE AND IRREVERSIBLE KINETICS COMBINED

Parameter values for the simulation of two different types of rotoviscometer tests on f-MFT shown in Sections 3.2 and 3.3 are listed in Table 1. Mizani et al., (2017) flocculated MFT with polymer: 800 g/tonne. After being flocculated with polymer, the material was left to rest for 30 minutes and bleed water was decanted. Because of the likely floc size, Mizani applied a vane-in-cup measuring configuration (Anton Paar Physica MCR301, Cup CC27, radius 14.46 mm, vane diameter 22 mm, height 40 mm, possibly ST 22-4V-40). When the vane was inserted in the sample, the rheological test commenced within 1 minute. In applying a vane fixture, the fluid shear rate is not as well-defined as in the bob-cup configuration, but wall slip might be an issue with bob-cup elements at low shear rates.

In our simulation, the value of the initial structure λ_i is chosen to be relatively high but smaller than 1. In that case, growth and decay are possible with respect to the initial conditions. The numerical value of irreversible shear break down parameters is of the same order as in Section 2.2. We elaborate on the fitting in Sections 3.2 and 3.3.

Table 1

Parameters for simulation rheological behaviour of flocculated tailings with Houska thixotropy model in combination with irreversible shear down of rheology

Parameter	symbol	value	unit
initial reference structure at $t=0$	λ_i	0.7	[-]
Sheared down maximum structure	$\lambda_{0\infty}$	0.1	[-]
Cum. Energy dissipation at 63% shearing down	E_{63}	300	[kJ/m ³]
Yield stress (at $\lambda=0$)	τ_c	20	[Pa]
Plastic viscosity (at $\lambda=0$)	μ_p	0.3	[Pa s]
Yield stress (at $\lambda=1$)	τ_0	800	[Pa]
Increment of viscosity (at $\lambda=1$)	c	20	[Pa s]
Reciprocal of recovery time-scale floc structure	a	1/3	[1/s]
Constant for reversible shear down	b	0.02	[-]
Reference shear rate in viscosity regularization	$\dot{\gamma}_0$	1	[1/s]
Inertia lag rotoviscometer	I	0.2	[s]

3.2. CREEP TESTS AND THEIR SIMULATION

A creep test is a test where the shear stress is held constant by the instrument and the instrument adapts its rotational velocity for mechanical balance. A series of such tests on bentonite and associated simulations, is for instance, reported by Roussel et al., (2004).

The results of creep test on f-MFT Mizani et al., (2017) as well as their simulations are shown in Figure 3. The graph basically shows apparent viscosity as a function of time.

Apparent viscosity is defined as: $\mu_a = \tau / \dot{\gamma}$. In all these graphs, the sequence of the listing in the legend is the same as the sequence of curves in the graphs.

We see an initial increase in all measurements in Figure 3. Mizani's et al. simulation model, Figure 3, "explodes" at high apparent viscosities, because no viscosity regularisation is applied (as seen at ~ 10 s).

Using the proposed model in Section 2, we attempt to simulate the measurements of Mizani et al., (2017). Results are shown in Figures 3 and 4. At 100, 200, 300 and 400 Pa imposed shear stress, the conditions are in the viscosity regularization region associated with a rheology characterised by an initial yield stress of 556 Pa (at initial structure $\lambda_i=0.7$). Here the shear rate is low, and therefore irreversible shear-down is negligible. The structure

grows, Figure 4, since the initial structure $\lambda_i < \lambda_0$. The conditions are then shifting to CSC's of higher structure: with the result that the apparent viscosity increases, giving similar trends, but not continuing, since $\lambda=1$ is reached, unlike that measured by Mizani et al., 2017.

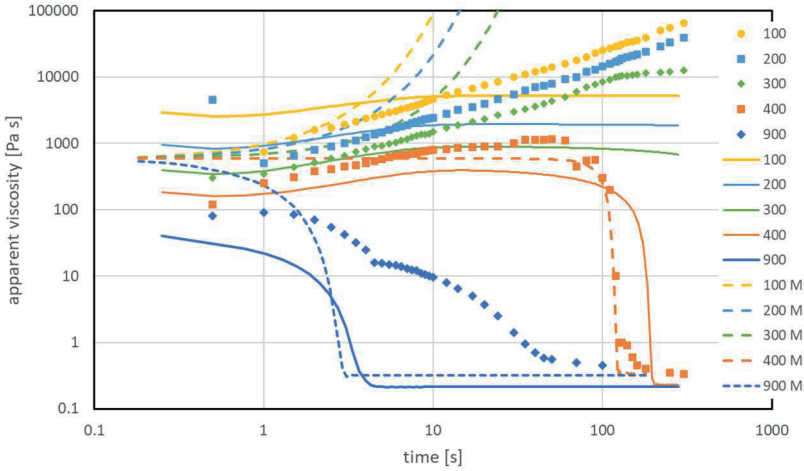


Figure 3 Mizani et al. 2017 apparent viscosity data (symbols) in creep tests and simulation (curves) after Mizani et al. 2017 (- -) and by the Houska model (continuous curves) (parameter values in Table 1, legend: imposed shear stress [Pa])

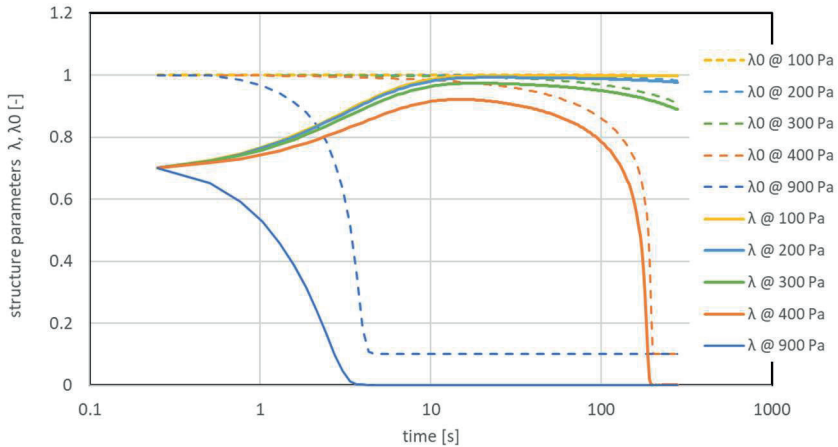


Figure 4 Structure parameters λ and λ_0 as a function of time for the Houska calculation shown in Figure 3. Constant shear stresses in the creep tests are given in legend: 100 to 900 Pa

The Houska model calculates different viscosities, starting from the beginning. This is not the case with the model used by Mizani et al., (2017) Because of the fluid mechanical approach, it was decided not to try to improve the simulation of the elastic part.

At a 400 Pa imposed shear stress, the conditions are close to bifurcation, where a low or high viscosity branch may develop with time. Figure 4 shows that the internal structure collapses after about 100 [s].

At a 900 Pa imposed shear stress the initial condition is well above the yield stress (556 Pa at $\lambda_i=0.7$). The associated shear rate can be found only at high shear rates. At the same time, the structure is irreversibly sheared down significantly, as governed by Eq.(2) and (3).

It is concluded that, essentially, the proposed model shows similar behaviour as measured and gives similar results as the simulation model of Mizani et al. (2017). These creep tests helped to set the conditions for the upper bound (τ_0, λ_i) for the Houska thixotropy model.

3.3. SEQUENCE OF CONTROLLED STRESSES AND SIMULATION

Using the same material as in the creep tests, Mizani et al. (2017) also conducted a series of shear stress step-down tests (800 Pa step-wise decreasing to 25 Pa). Such tests may give the EFC branch, when the material is given sufficient time to equilibrate, except for a declining EFC branch which is inherently unstable at constant shear stress conditions. Mizani concluded that the lowest attainable shear stress in the flow curve was 50 [Pa]. At lower shear stresses, the material solidified again. This 50 [Pa] would correspond to the minimum in the EFC shown in Figure 2. This also means that the lower yield stress τ_∞ of the thixotropy model should be smaller than this value (fitted value 20 Pa, Table 1). Measurements and simulations by Mizani et al. and by the Houska model are shown in Figure 5. In our Houska based simulation, the irreversible part is already totally sheared down in the first 5 seconds, as indicated by λ_0 . This part of the simulation is governed by the value of $E_{63\%}$ for irreversible shear down, Table 1.

As in the 900 Pa shear stress test shown in Figures 3 and 4, the material is sheared down quickly. If in down-sheared low viscosity consistency, the imposed shear stress is below the minimum shear stress of the EFC curve, the associated asymptotic condition is again in the strengthened steep part of the flow curve's viscosity regularization branch, where apparent viscosity increases again. This happens at around 26 s.

From these simulations, it is concluded that rheological tests to quantify equilibrium flow curves of freshly flocculated tailings should preferably be conducted with minimal energy input into the sample.

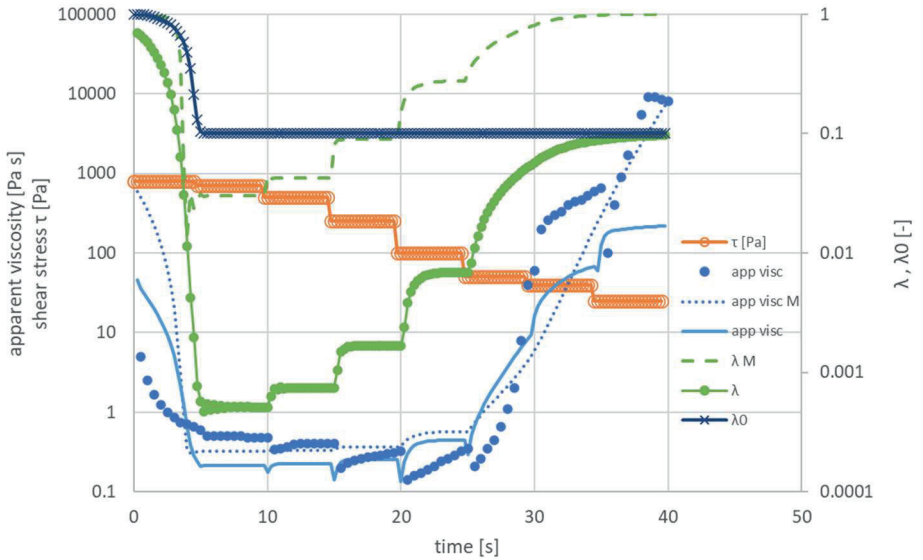


Figure 5 Simulation of stepped-down shear stress test (800, 700, 500, 250, 100, 50, 40 and 25 Pa), Mizani et al. 2017 rheometric data (single dots) a simulation with Mizani's thixotropy model (M: dotted & striped) and with the Houska thixotropy model

4. RHEOMALAXIS IN FLUID FLOW DOWN A BEACH

With flocculation it is important to understand the consequences of the flow behaviour. The flocculated strength is very high, leading to unrealistic large flow depths. So, the research question is: what happens when the material flows down the beach? Does it create a weakened bottom layer because of its own localized shear? If so, does it shear down all the way, and will the flow depth and velocity be governed by the remoulded sheared down properties?

With flocculation the magnitude of irreversible time-dependency is larger than reversible time-dependency. To investigate the consequences of polymer addition on the tailings flow, we conducted exploratory CFD calculations addressing the dominant irreversibility only. The kinetic equation for the irreversible part becomes in that case, compare with Eq. (1):

$$\frac{D\lambda_0}{Dt} = -(\lambda_0 - \lambda_{0,\infty}) \frac{\tau}{E_{63}} \dot{\gamma} \quad (5)$$

Notice that b of Eq. (1) is replaced by local shear stress τ divided by characteristic cumulative dissipation E_{63} . When the minor irreversible part is also encompassed $\lambda_{0,\infty}=0$, the structure of the RHS term is the same as the last term in the right-hand side of Eq(1). Hence, we may conduct an exploratory calculation with the CFD model of Talmon et al.

(2023), using Eq. (1), but nullify the recovery time. Using this existing code, we cannot connect to local shear stresses, as per Eq. (5), but we take a representative value.

With $\tau = 100$ Pa, we exploratively investigate what the role of irreversible shear down on beach flow of f-MFT might be. In this case, the value of b is: $100/300 \text{ E-3} = 0.0003$, i.e., substantially smaller than b of the reversible part (Table 1), but of similar order as applied in the time-reversible calculations in Talmon et al. (2023). Calculations were conducted for discharge flow rates at the inlet of 0.1, 0.2 and 1 $[\text{m}^2/\text{s}]$. The parameter settings for the calculations are listed in Table 2.

Table 2

Parameters for the simulation of beach flow of f-MFT (Mizani et al. 2017 data)

Houska model	value	
yield stress (at $\lambda = 0$): $\tau_{v,\infty}$ [Pa]	20	
plastic viscosity (at $\lambda = 0$): μ_∞ [Pa s]	0.3	
yield stress (at $\lambda = 1$): τ_0 [Pa]	800/120	full/reduced
viscosity increment ($\lambda = 0$ to 1): c [Pa s]	20	
structure self-recovery: a [1/s]	0.0	
structure shear breakdown: $b = \tau/E_{63\%}$ [-]	0.0003	
viscosity regularisation: m [s]	1,000	
initial $\lambda_i = 0.7$, inlet $\lambda_i = 0.7$, $i=0.02$	grid 128*32	vert. str'ch: 10

If the material remains at its augmented strength, with 560 [Pa] at $\lambda_i=0.7$ as maximum yield stress, one would expect a layer thickness of at least 1.9 m on a slope of $i=0.02$ (and density of 1500 kg/m^3 , static calculation). But in our CFD calculation at $q=1 \text{ m}^2/\text{s}$ we are finding a layer thickness of about 1 m, which is still substantial. The structure has been sheared down at the bottom. It is more realistic to evaluate at lower flow rates (wider flow) and an initial lower strength, assuming upstream degradation by hydraulic transport or plunge pooling. An overview of calculated depths is given in Table 3 and an example of the calculated flow is given in Figure 6. CFD calc's without thixotropy give the same flow depths as per theory.

Table 3

Calculated flow depth beach flow

condition	theory unremoulded, $\lambda_i = 0.7$	CFD	theory remoulded $\lambda_i = 0.0$
$q = 1 \text{ m}^2/\text{s}$, $\tau_0 = 800$ [Pa]	2.2 m	~1 m	0.18 m
$q = 0.2 \text{ m}^2/\text{s}$, $\tau_0 = 800$ [Pa]	2.0 m	~0.7 m	0.13 m
$q = 0.2 \text{ m}^2/\text{s}$, $\tau_0 = 120$ [Pa]	0.52 m	~0.37 m	0.13 m
$q = 0.1 \text{ m}^2/\text{s}$, $\tau_0 = 120$ [Pa]	0.46 m	~0.33 m	0.114 m

We see instabilities arising at $q=0.1$ and $0.2 \text{ [m}^2/\text{s}]$. Puffs of low structure are swept away from the bottom area, and the tailing surfaces level varies in concert. Rheomalaxis has no self-recovery mechanism, that could provide a stabilizing role. We conclude that the shear in the boundary layer lowers the structural level and therefore the viscosity, but

is insufficient to decrease the viscosity due to the remoulded conditions in the boundary layer.

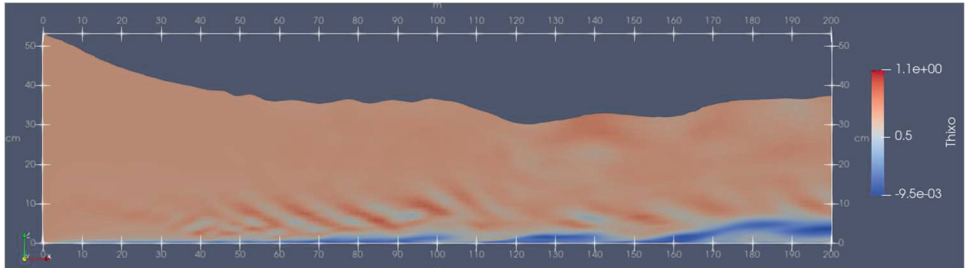


Figure 6 Structure “thixo= λ ” by rheomalaxis for $q=0.1 \text{ m}^2/\text{s}$, captured after 60 minutes

We have shown that the Houska model is capable too of simulating viscosity bifurcation behaviour. Our fitting in the current paper was done on the basis of previously conducted controlled shear stress (CSS), tests emphasizing bifurcation, but the experience is that the parameter values can also, and more easily, be obtained with controlled shear rate (CSR) tests, supplemented by a CSS test, Talmon et al., (2021a).

Two alternative ways to capture the rheological time-dependency of oil sands in flow calculation have now been explored: reversible (Mizani et al., Talmon et al., 2023) and a combination of partly reversible and irreversible (current paper). Both approaches are able to mimic existing rheometry tests, but incorporation of rheomalaxis seems the more appropriate, as it is consistently reported for polymer amended tailings. A consequence of rheomalaxis is the formation of a lubricating layer, lowering hydraulic resistance, but irregular flow seems to be triggered.

5. CONCLUSIONS

The Houska time-dependent consistency model incorporating the distinct yield stresses of structured fluid is capable of mimicking the viscosity bifurcation behaviour when it includes viscosity regularisation, which is a necessity when coping with yield stresses in fluid flow calculations anyway.

The Houska model is modified to include reversible and irreversible rheological behavior typical for polymer amended materials. Fitting results for the constitutive model are similar to those obtained using the Mizani et al. model, which was originally fitted to these data.

In a fluid flow model, it has to be implemented, as a full suite:

- structure parameter λ as a scalar as a measure of reversible flocculated structure.
- a scalar transport function for cumulative shear energy dissipation E as a measure of irreversible shear down of rheology, which governs and sets the maximum attainable structure in the Houska model.

The Houska model forms a transparent starting point for the fluid flow profile calculations, the stability analysis of flow, and the formation of sedimentary deposition patterns when time-dependency is taken into account.

By incorporating rheomalaxis in a CFD calculation of tailings disposal on a beach, it is found that a lubricating layer is formed, reducing flow depth. Irregular flow develops after some distance.

ACKNOWLEDGEMENTS

Thanks to Prof J.C. Winterwerp for contributing ideas and discussions. Dr ir M. Nabi for advising on the CFD model. IOSI tailings research motivated the study of thixotropy.

REFERENCES

1. Diep, J., Weiss, M., Revington, A., Mayls, B., Mittal, K., 2014. In-line mixing of mature fine tailings and polymers. Paste 2014 conference AGU.
2. Gillies, R., Spelay, R., Sun, R., Godsall, A., Li, C., 2012. Pipeline transport of thickened oil sand tailings. IOSTC, Edmonton.
3. Hewitt, D.R., Balmforth, N.J., 2013. Thixotropic gravity currents. *J. Fluid Mech.* (2013), vol. 727, pp. 56-82.
4. Houska, M., 1981. Engineering Aspects of the Rheology of Thixotropic Liquids. PhD-thesis, Czech Technical University, Prague.
5. Meshkati, E., Talmon, A.M., Luger, D., Bezuijen, A., 2021. Rheology of clay rich soft sediments: from fluid to geo-mechanics. Proc. Dredging Days 2021, sept 28-29th, on-line.
6. Mietta, F., Chassagne, C., Winterwerp J.C., 2009. Shear induced flocculation of a suspension of kaolinite as function of pH and salt concentration. *Journal of Colloid and Interface Science* 336 (2009) 134–141.
7. Mizani, S., Simms, P., Wilson, W., 2017. Rheology for deposition control of polymer-amended oil sands tailings, *Rheol Acta*. DOI 10.1007/s00397-017-1015.
8. Moore, F., 1959. The rheology of ceramic slips and bodies. *Transactions British Ceramic Society*, Vol. 58, 470-494.
9. Neelakantan, R., Vaezi, F.G., Sanders, R.S., 2018. Effect of shear on the yield stress and aggregate structure of flocculant dosed, concentrated kaolinite suspensions. *Minerals Engineering*, Vol. 123, 95-103.
10. Roussel, N., Le Roy, R., Coussot, P., 2004. Thixotropy modelling at local and macroscopic scales. *Journal of Non-Newtonian Fluid Mechanics.* (117):85-95.
11. Salinas, C., Martinson, R., Cooke, R., Ferrada, O., 2009. Shear and Rheology Reduction for Flocculated Thickened Tailings. Paste 2009.
12. Sun, Y., 2018. Recovery of thickened kaolinite suspension properties through shear. MSc-thesis, University of Alberta, Canada.
13. Talmon, A.M., Hanssen, J.L.J., Winterwerp, J.C., Sittoni, L., van Rhee, C., 2016. Implementation of Tailings Rheology in a Predictive Open-Channel Beaching Model. Paste 2016 conference AGU.
14. Talmon, A.M., Meshkati, E., Lelieveld, T., Goda, A.P.K., 2021a. Evaluation of Houska thixotropic model for quantification of shear and time dependency of different mud types. Proc. Dredging Days 2021, sept 28-29th, on-line.
15. Talmon, A.M., Meshkati, E., van Kessel, T., Lelieveld, T., Goda A.P.K., Trifkovic, M., 2021b. On thixotropy of flocculated mature fine tailings: rheometry and lumped structure parameter modelling. proc. Tailings and Mine Waste conf., Nov. 7- 10th, 2021, Banff, Canada.
16. Talmon, A.M., Meshkati, E., Nabi, M., Simms, P., Nik, R.M., 2023. Comparing various

thixotropic models and their performance in predicting flow behaviour of treated tailings. *Paste* 2023.

17. Toorman, E.A., 1997. Modelling the thixotropic behaviour of dense cohesive sediment suspensions, *Rheol Acta* 36:56-65.
18. Worrall, W.E., Tuliani, S., 1964. Viscosity Changes during the Ageing of Clay-Water Suspensions. *Trans Brit Ceramic Soc* 63:167–185.
19. Winterwerp, J.C., 2017. personal communication.

